Absolute measurements of the triplet-triplet annihilation rate and the charge-carrier recombination layer thickness in working polymer light-emitting diodes based on polyspirobifluorene

C. Rothe,* H. A. Al Attar, and A. P. Monkman
Department of Physics, University of Durham, Durham DH1 3LE, England
(Received 26 April 2005; revised manuscript received 18 July 2005; published 27 October 2005)

The triplet exciton densities in electroluminescent devices prepared from two polyspirobifluorene derivatives have been investigated by means of time-resolved transient triplet absorption as a function of optical and electrical excitation power at 20 K. Because of the low mobility of the triplet excitons at this temperature, the triplet generation profile within the active polymer layer is preserved throughout the triplet lifetime and as a consequence the absolute triplet-triplet annihilation efficiency is not homogeneously distributed but depends on position within the active layer. This then gives a method to measure the charge-carrier recombination layer after electrical excitation relative to the light penetration depth, which is identical to the triplet generation layer after optical excitation. With the latter being obtained from ellipsometry, an absolute value of 5 nm is found for the exciton formation layer in polyspirobifluorene devices. This layer increases to 11 nm if the balance between the electron and the hole mobility is improved by chemically modifying the polymer backbone. Also, and consistent with previous work, triplet diffusion is dispersive at low temperature. As a consequence of this, the triplet-triplet annihilation rate is not a constant in the classical sense but depends on the triplet excitation dose. At 20 K and for typical excitation doses, absolute values of the latter rate are of the order of 10^{-14} cm^3 s^{-1}.

DOI: 10.1103/PhysRevB.72.155330 PACS number(s): 78.66.Qn, 78.55.−m, 33.50.Dq

INTRODUCTION

The active polymer layer is the centerpiece of a polymer light-emitting diode, which must allow for a balanced charge-carrier injection as well as exhibit decent transport properties for both electrons and holes. Following charge-carrier recombination, in the best case, the subsequently created singlet exciton decays radiatively and thus contributes to the sample emission. However, for pristine polymers, three-quarters of the recombination events initially lead to the formation of nonemission triplet excitons.[1] Though dominant, this is by far not the only loss mechanism for pristine polymer light-emitting diodes. Additionally, unbalanced electron and hole injection may lead to dark currents.[2] To circumvent this, one could either match the electrode materials to the highest occupied molecular orbital (HOMO) and lowest unoccupied molecular orbital (LUMO) level of the polymer or chemically modify the polymer itself toward the energy levels of the given electrodes, typically ITO and a low work-function metal.[3] Even if balanced injection is achieved, any significant difference between the electron and hole mobility (a commonly observed situation[4]) would result in a charge-carrier recombination zone that is located close to the electrode that injects the low mobility carrier. Again this may open quenching pathways and thus lower the quantum efficiency of the device.[5] Therefore in the ideal scenario, electrons and holes are injected in equal proportions and meet each other in the center of the active polymer layer. Alternatively, the charge-carrier recombination zone for multilayer devices may be engineered by choice of the appropriate layer materials.[6] However, such a device structure is difficult to put into practice when using the cost-effective ink-jet printing technique. On the other hand, there is no reliable method so far for measuring the position and width of the charge-carrier recombination layer in single-layer devices. Potentially, one could measure the ratio of electron and hole mobility and in this way infer the position of the recombination layer from the active layer thickness. In this context, the commonly employed time-of-flight (TOF) technique is only capable of probing the mobility of one of the two charge carriers. Even so, this method demands great skills from the experimentalist as the results obtained are often unreliable. Therefore, at present the device performance is optimized by a trial-and-error method rather than a true measurement. Alternatively, one could turn to a new optical method in order to achieve the charge-carrier layer thickness.

For high triplet generation doses both optically and electrically excited, bimolecular triplet annihilation is the dominant decay mechanism of the triplet exciton in polyfluorene derivatives.[7–9] If the triplets are immobile, which is the case at low temperature,[7,8] then triplet-triplet annihilation will be most efficient within the triplet generation layer, which for electric excitation is identical to the charge-carrier recombination layer. Therefore, the layer thickness is a natural parameter that influences the steady-state triplet density at low temperature and the layer thickness itself can be gained from an analysis of the triplet density as a function of the excitation dose. The triplet density after optical and electrical excitation may be probed by observing the phosphorescence intensity.[8,10] However, with the latter method the data are taken pointwise, which is very time-consuming. It is more efficient to measure the buildup of the triplet density during continuous excitation by means of transient triplet absorption detection. In this way, time essentially parametrizes the excitation dose, and each curve contains a whole range of doses. Here we demonstrate how this technique can be used to obtain accurate recombination layer thicknesses by means

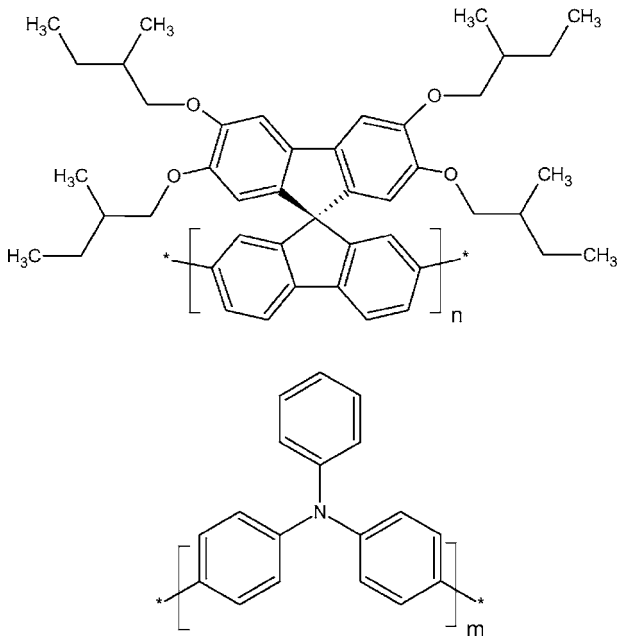

FIG. 1. Chemical structures of the investigated polymers. Above: Repeat unit of the polyspirobifluorene homopolymer; below: the TAD-type hole transport moiety that is randomly incorporated in the above polymer backbone for the copolymer.

of a representative conjugated polymer, and in a further application we show that balancing the charge-carrier mobilities of this polymer yields a wider recombination layer.

EXPERIMENTAL

In this study, we investigate two types of blue emitting electroluminescent devices based either on pristine polyspirobifluorene (homopolymer) or on a very similar copolymer which exhibits improved hole injection and transport properties by means of randomly chemically bound triphenylamine moieties (TAD) within the polyspirobifluorene backbone.[6,11] All chemical structures are depicted in Fig. 1. As a consequence of the spiro-linkage, both these polymers are inert against backbone oxidation, which otherwise results in the formation of weakly emissive defect sites associated with fluorenone.[12] Thus, with special regard to electrical excitation, we investigate genuine polymer properties rather than effects associated with electrons trapped in such keto-defect sites.

The polymer devices were provided by Philips Research Eindhoven and details about their fabrication are given elsewhere.[13] Briefly, the diode structure is comprised of a ITO/PEDOT:PSS [poly-(3,4-ethylenedioxythiophene):poly-(styrenesulforic acid)] anode, the 80 nm spin-coated polymer layer (90 nm for the copolymer), and the evaporated Ba/Al cathode (5 nm barium capped with 100 nm aluminum). Before leaving the nitrogen atmosphere, the devices were finished using a getter and a permanently sealed metal cap in order to protect the cathode from water and oxygen.

All experiments were performed at 20 K, with the device being mounted onto the cool finger of an optically and electrically accessible closed cycle displex helium cryostat. A 25 mW continuous-wave 400 nm laser diode module (Laser2000) was employed to photoexcite the active area of the device (3 mm diam) perpendicular to the sample surface. Here, a neutral density filter wheel allowed to attenuate the excitation power, which was measured using an OPHIR power meter. A 100 W HP current pulse generator provided the electrical excitation.

The triplet exciton density was probed close to the maximum of its corresponding transient absorption spectrum using a 50 mW 785 nm laser diode module (Laser2000). This probe beam was focused onto the active area of the device, reflected by the cathode, passed through an appropriate cut-off filter to reject sample emission, detected by a Si photodiode combined with a 200 MHz transimpedance amplifier (Femto), and monitored by a 1 GHz Oscilloscope (Agilent). Hence, all original transient absorption data have the units volts V. The experiment was repeated with a frequency of 0.2 Hz in order to allow for a sufficient triplet decay between the subsequent excitation pulses, and at least 100 excitation pulses were accumulated for one dataset. In doing so, changes in the transient absorption ($\Delta T/T$) of 10^{-4} with a temporal resolution of 10 ns could be measured. Importantly, all measurements on a single device were made under identical conditions, i.e., there was no need to change the geometry of the setup in order to switch between optical and electrical excitation mode.

The device emission consisting of fluorescence and phosphorescence has been measured by means of a fast and sensitive setup based on a gated CCD camera (4Picos, Stanford Computer Optics), which probes the dispersed sample emission as a function of time. Details for this setup are given elsewhere.[8]

Ellipsometric data were acquired with a variable angle spectroscopic ellipsometer (VASE™, J.A.Woollam) of the rotating analyzer type. All measurements were performed in air at room temperature for two angles of incidence 65° and 75°, and in the wavelength range of 200–1000 nm in steps of 10 nm. In order to increase the accuracy of the modeling for both polymers, a range of samples possessing different layer thicknesses were characterized independently. Spectroscopic ellipsometry data for blank Si/SiO_2 substrates were acquired as well and the thickness of the SiO_2 layer determined. These substrate properties were applied to model the polymer system. From several previous studies on similar polyfluorene derivatives,[14,15] it is known that the polymer chains arrange themselves predominantly in the plane, i.e., parallel rather than perpendicular to the substrate surface during the spin coating. This leads to an anisotropic structure that is uniaxial with the optical axis in a specific direction. Measurements at different azimuth angles indeed indicate that our samples were symmetric with respect to rotation about the surface normal. Therefore, we assume our samples to be uniaxial with the optical axis perpendicular to the sample surface and both polar and azimuth angles are set to zero during the fitting procedure. As shall be shown, our main interest within the present study is to accurately determine the ordinary optical constants, therefore only thin samples below 80 nm were considered. The anisotropic characteristics of such samples are very weak and a simple uniaxial model con-

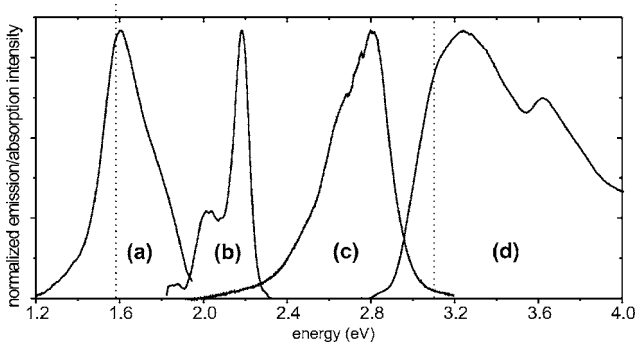

FIG. 2. Some spectra of the copolymer including transient triplet absorption (a), phosphorescence (b), prompt fluorescence (c), and absorption spectra (d). The dashed lines indicate the optical excitation and the transient absorption probe energy, respectively.

structed from ordinary and extraordinary optical constants (subscripts o and e, respectively) using the Cauchy equation $n_{o,e}(\lambda)=A_{o,e}+(B_{o,e}/\lambda^2)+(C_{o,e}/\lambda^4)$ to model the wavelength-dependent ordinary and extraordinary refractive index. Here, A is called the coefficient of refraction and B, C the coefficients of dispersion.[16] The fitting was first achieved for the spectral range 550–1000 nm where the absorption of both polymers is negligible. With all Cauchy parameters plus the polymer layer thickness being variable, an excellent global fitting was obtained. The mean-square error (MSE) and the correlation matrix were examined to insure the independence of the ordinary relative to the extraordinary optical constants. Thickness and Cauchy parameters were then fixed and the ordinary and extraordinary optical constants (n and k) independently fitted successively extending into the absorption region. We note here that this method is only applicable to thin samples where both $\lambda^{\mathrm{opt}}d$ (λ^{opt} is the absorption coefficient and d the sample thickness) and the z component of the anisotropy have a weak influence on the propagation of the electromagnetic field.

RESULTS AND DISCUSSION

Shown in Fig. 2 are some characteristic spectra of a copolymer thin film including room-temperature absorption ($S_0 \rightarrow S_1$) and excited-state triplet absorption ($T_1 \rightarrow T_n$) as well as low-temperature prompt fluorescence ($S_0 \leftarrow S_1$) and phosphorescence ($S_0 \leftarrow T_1$). These data are very similar to the corresponding homopolymer spectra that have been published recently,[1] which suggests that the TAD moieties of the copolymer have no major influence of the photophysics of polyspirobifluorene as such.

Figure 3 shows the buildup of the triplet density during both electrical and optical continuous excitation by means of time-resolved transient triplet absorption. Here, an initial linear rise of the triplet density smoothly turns into a saturation regime. Furthermore, following the excitation pulse the triplet density decays much faster as compared to the monomolecular triplet lifetime, which at 20 K is about 1 s.[8,17] Consistent with foregoing work on polyfluorene derivatives,[7–10] both these observations verify that the triplet density within the device is subject to bimolecular triplet annihilation,

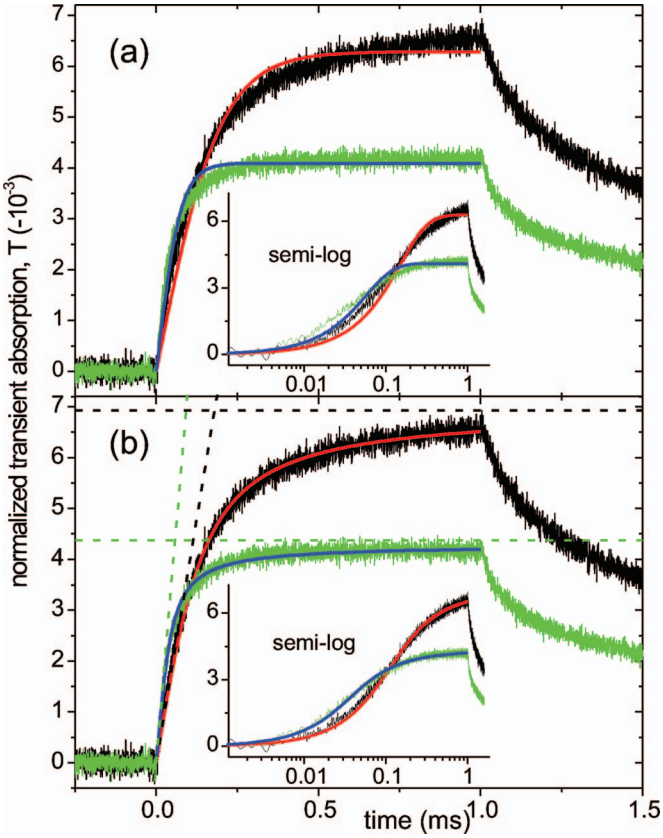

FIG. 3. (Color) Two typical time-resolved induced absorption datasets for the homopolymer during optically (30 mW/cm^2, black) and electrically (6 V, green) exciting the device for 1 ms. In order to better evaluate the initial time region, the insets show the same data in a semilogarithmic fashion. In part (a), simulations according to the homogeneous triplet generation model, Eq. (2), are included as red and blue solid lines. Similarly, part (b) contains fits to the inhomogeneous triplet generation model, Eq. (5). For the latter case, the obtained initial slopes and the steady-state values are shown as dotted and dashed straight lines, respectively.

which in our experimental situation clearly emerges as the main decay path for the triplet excitons. In this framework, the time dependence of the triplet density or the shape of the observed transient triplet absorption curves, respectively, contains information about the nature of triplet-triplet annihilation, in particular of its associated rate constant, γ_{TT}.

Thus, we set out to simulate the measured graphs using an appropriate model, which then allows us to extract parameters of physical relevance. The starting point is the rate equation for the triplet generation without the monomolecular decay term. Such a treatment is legitimate as long as the considered time span is much smaller than the monomolecular triplet lifetime ($t \ll 1$ s). Initially, and in common with all classical treatments, it is assumed that the triplet generation occurs homogeneously throughout the active layer,

$$\frac{dI(t)}{dt} = I_0 - \gamma_{\mathrm{TT}}[I(t)]^2 \tag{1}$$

with I_0 being the triplet generation rate. This yields the time-dependent triplet density, $I(t)$, as

$$I(t) = \sqrt{\frac{I_0}{\gamma_{TT}}}\tanh(t\sqrt{I_0\gamma_{TT}}). \quad (2)$$

Within this model, the observed initial slope and the corresponding saturation level are directly proportional to I_0 and $\sqrt{I_0}$, respectively. This, however, is inconsistent with the experimentally observed curves shown in Fig. 3. In this special situation, the green dataset (electric excitation) rises relatively faster than the black one (optical excitation). However, the latter, slower rising, curve finally approaches a higher steady-state value. Such a behavior cannot be explained by Eq. (1). Thus, it is not astonishing that simulations according to Eq. (2) fail to reproduce the observed graphs. For all datasets, the initial rise is underestimated [see the semilogarithmic inset of Fig. 3(a)] and the turnover into the saturation regime occurs too early.

Subsequently, a more realistic scenario is discussed. We assume that the triplet excitons are mainly generated in a thin layer with an exponential density profile rather than homogeneously throughout the whole thickness of the device. The logic behind this is immediately clear for optical excitation as here the penetration depth is an exponential function characterized by λ^{opt}. Thus, initially for optical excitation the triplet density is higher at the ITO surface of the device. A similar situation also holds true for electrical excitation. Here, the carrier mobility for all common conjugated homopolymers is generally unsymmetrical.[4] In the present situation, the homopolymer polyspirobifluorene is an electron transporting material.[18] Therefore, the carrier recombination is expected to take place close to the anode interface where the less mobile holes are injected. Though little is known, here the thickness profile of this charge-carrier recombination zone shall also be described by an exponential function, characterized by λ^{el}. Thus, the triplet (and simultaneously the singlet) generation rate is supposed to be higher in the area close to the ITO anode and exponentially diminishes toward the cathode surface. The above arguments are of special importance as at low temperature [for the materials studied here $T<60$ K (Ref. 19)] the triplet diffusion is dispersive,[8] which means that after a few downhill jumps in energy, the triplet excitons become essentially trapped within the intrinsic density of energetic states (DOS).[20] Besides, such inefficient migration is accompanied by a triplet-triplet annihilation efficiency that is reduced relative to room temperature,[8] which is in fact the reason why low temperature has been used throughout. Immobile triplets imply that the initial inhomogeneity of the triplet generation cannot be compensated by migration and thus is preserved during the whole triplet lifetime. From the aforementioned it follows that the absolute number of triplet excitons annihilating each other depends on the sample depth, x, relative to the triplet generation surface, which in our case is the anode for both excitation modes.

Quantitatively, the rate equation is modified to

$$\frac{dI(x,t)}{dt} = I_0\lambda e^{-\lambda x} - \gamma_{TT}[I(x,t)]^2, \quad (3)$$

where $I_0\lambda e^{-\lambda x}$ denotes the triplet generation at a sample depth x. It is now important to remember that the overall triplet-triplet annihilation is proportional to the sum of the individual layers at a certain sample depth x, rather than to the overall triplet density. Therefore, in order to find the overall triplet density $I(t)$, first Eq. (3) has to be solved for each polymer layer x followed by integration over all x. Note again that this treatment is only legitimate as long as the triplets are immobile. As the triplet generation is independent of time, the solution of Eq. (3) is identical in its structure to Eq. (2) and essentially describes the time-dependent triplet density limited by bimolecular annihilation for an infinitesimally thin layer of the device at a distance from the surface x. Then, the overall triplet density, as experimentally probed, is given by

$$I(t) = \frac{2}{\gamma_{TT}\lambda t}\ln\cosh(t\sqrt{I_0\lambda\gamma_{TT}}). \quad (4)$$

This relation holds true if the triplet generation layer (both for optical and electrical excitation) is much smaller than the sample thickness. The slope of the above equation at time zero is given as $dI(t\to 0)/dt = I_0$ and simply reflects the fact that at early times the triplet density follows the triplet generation rate, as here bimolecular annihilation is not yet active. In line with intuitive reasoning, the initial rate is independent of $\lambda^{el/opt}$. Hereafter, the superscripts "el" and "opt" refer to electric and optical excitation, respectively. For steady-state conditions, Eq. (4) yields $I(t\to\infty) = \sqrt{4I_0/\lambda\gamma_{TT}}$. In common with the classical treatment (homogeneous triplet generation), this time-independent triplet density is proportional to the square root of the quotient of generation and annihilation rate. Unlike the classical value, for inhomogeneous triplet generation the absorptivity also occurs in the steady-state value as the latter is proportional to the square root of the absorption layer thickness. For example, a thinner recombination zone yields a smaller steady-state value for the triplet density. Again this is intuitively clear as a thin layer with high absorption coefficient leads to high triplet densities accompanied by high bimolecular annihilation efficiencies; essentially this thin zone shields the incoming excitation flux from a deeper penetration into the sample. The dependence of the steady-state triplet density on the triplet generation layer thickness now allows us to clarify the at first glance puzzling observation of Fig. 3. Remember, here a higher triplet generation rate of the electrically excited curve is accompanied by a lower steady-state value relative to the optical one, respectively. From Eq. (4), one now concludes that $\lambda^{el} > \lambda^{opt}$, i.e., the charge-carrier recombination layer is smaller than the light penetration depth at the excitation wavelength.

To gain further quantitative insight, we first note that Eq. (4) yields λ and γ_{TT} for any individual experiment not as independent, free parameters. Therefore, it is convenient to rewrite Eq. (4) as

$$\varepsilon I(t) = \frac{\Delta T(t)}{T} = \frac{2}{ta}\ln\cosh(tc) \quad (5)$$

with $a = \lambda\gamma_{TT}/\varepsilon$ and $c = \sqrt{\lambda\gamma_{TT}I_0}$. Here we have additionally introduced the quantity ε, which denotes the constant of proportionality between the true triplet density $[I(t)]$ and the

experimentally measured normalized change in transient triplet absorption $[\Delta T(t)/T]$. In particular, with respect to optical and electrical excitation, for our experiments there is only one ε, because the transient triplet absorption was always measured under unchanged experimental conditions. Thus, the electrical and optical datasets are in a fixed relative ratio to each other. This condition implicitly assumes identical triplets after electrical and optical excitation. This general knowledge was confirmed by measuring the energetic position (phosphorescence spectra) as well as the radiative lifetime of the triplet excitons. Here, in both cases and for both polymers no significant alterations with the different excitation modes were observed.

Similar to the homogeneous triplet generation model, least-squares fits according to Eq. (5) are shown in Fig. 3 as well. The improvement of the fit is clearly visible as now the simulations perfectly match the experimentally observed curves. Note, this has not been paid for by increasing the number of free parameters. In fact, both models [Eqs. (2) and (5)] rely on only two fitting parameters. In conclusion, Eq. (5) is the more appropriate model to describe the triplet density following both optical and electrical excitation at low temperature.

Now valuable information about working devices can be gained as the fitting parameters contain several material constants such as the charge-carrier recombination layer thickness for electrical excitation. Thus, in the following we set out to determine the recombination layer thicknesses $1/\lambda^{el}$ and the triplet-triplet annihilation constant, γ_{TT}, for both polymers by comparing optical and electrical parameters. Both these quantities can be extracted from the parameter $a=\lambda\gamma_{TT}/\varepsilon$. At first glance, a only depends on material parameters that are independent of excitation dose and as such should adopt only two values for each material, one for optical and one for electrical excitation. Then a simple comparison of these values allows one to define λ^{el} relative to λ^{opt}, the latter being independently measured using other techniques. However, instead of using only two single datasets, it is physically more solid to obtain the parameters a from a whole series of datasets dependent on triplet generation dose. To do so, we varied the optical excitation power and the driving voltage and fitted the measured data according to Eq. (5). Thus, we obtained the parameters a as a function of their corresponding (relative) triplet generation rates, εI_0. In Fig. 4, these data are plotted for the copolymer for both excitation modes. Surprisingly, a is far from being a simple constant, but instead depends on the (triplet) exciton generation rate. Within this double logarithmic presentation, the observed dependency is easily recognized as an algebraic function with an identical exponent for both optical and electrical excitation of 0.71. These at first glance puzzling observations are not inconsistent but in fact must be expected for the case of nonclassical, dispersive triplet migration, as shall be demonstrated in the following. To start with, we only consider the optical dataset. Beyond doubt, both the (inverse) penetration depth of the light, λ^{opt}, as well as the constant of proportionality, ε, do not depend on the excitation density. Therefore, we conclude that γ_{TT} is not an absolute constant in the classical sense but instead the rate of bimolecular triplet annihilation accelerates with increasing excitation dose. It

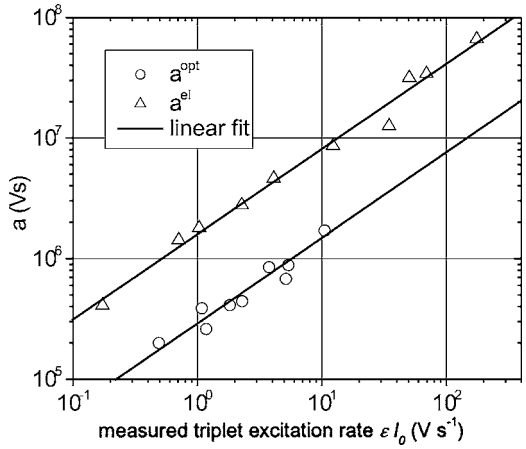

FIG. 4. Double logarithmic presentation of the copolymer parameter $a=\lambda\gamma_{TT}/\varepsilon$ for optical and electrical excitation vs the corresponding triplet generation flux as derived from simulations of the induced triplet absorption dependencies such as shown in Fig. 3. The solid lines represent least-square fits to both excitation modes. For guidance, the x axis roughly covers the range from 1.5 to 30 mW/cm^2 for optical and 5 to 7.7 V for electrical excitation.

has already been stated above that the triplet migration, which is rate-limiting for bimolecular annihilation, at the temperatures employed here is dispersive.[8] This naturally implies that γ_{TT} is not a constant but depends on time and this in turn renders γ_{TT} dependent on the triplet density.[21] To illustrate this point, consider a dispersive triplet diffusion that obeys an algebraic time dependence, $D(t)=D_0t^{-a}$, with a slope of $\alpha=-0.7$, i.e., the triplet migrates slower at longer times after its creation. The average distance traveled by the triplet until annihilation is given by $\Delta s=\int_0^T D(t)dt$, which yields the triplet lifetime as $T=[(1-\alpha)\Delta s/D_0]^{1/(1-\alpha)}$. If now the average traveled distance is halved by increasing the excitation dose appropriately, then it only takes a tenth of the previous time to overcome this separation rather than half the time as expected from classical diffusion ($\alpha=0$). Thus, in contrast to the classical treatment, in the dispersive diffusion regime the lifetime of the annihilating excitons does not scale linearly with the average distance between the triplets. Such effects have clearly been observed on isolated polymer chains (i.e., intrachain triplet-triplet annihilation) by means of excitation dose-dependent pulse radiolysis.[22] The reader is referred to Scheidler *et al.* for a more detailed analysis of this issue.[21] In conclusion, γ_{TT} depends on the triplet exciton density and might be described for the copolymer by $\gamma_{TT}(I_0)=\gamma_{TT}^0 I_0^{0.71}$.

This dependency may be cross-checked using laser dose-dependent measurements of the phosphorescence, i.e., the emission rather than the transient absorption of triplet excitons. In order to vary the triplet excitation dose, it is convenient to change the length of an optical excitation pulse, which, however, was chosen much shorter ($\leqslant$1 ms) as compared to the triplet lifetime ($\sim$1 s) and thus can still be considered as pulsed excitation. Exciting in this way rather than using short laser pulses of variable power has the advantage of avoiding any singlet-singlet annihilation, which otherwise might interfere with the triplet dose dependency.[23] Then,

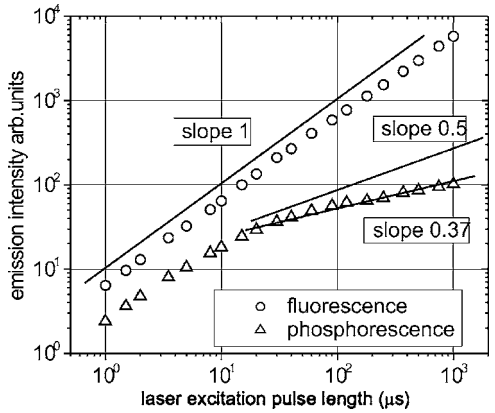

FIG. 5. Double logarithmic dependencies of the fluorescence intensity (during the pulse) and the phosphorescence intensity (100–800 ms after the pulse) as a function of the optical excitation pulse length at an excitation dose of 30 mW/cm^2 for the copolymer. The solid lines are guide lines with slopes as indicated.

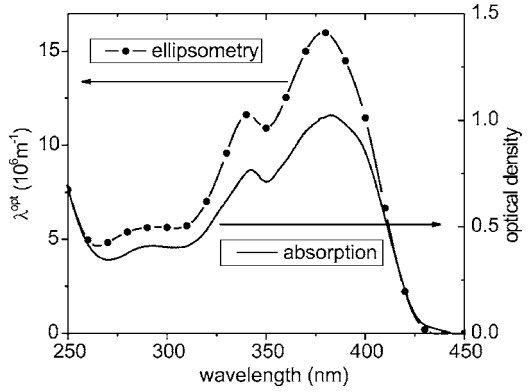

FIG. 6. Wavelength-dependent light penetration depth λ^{opt} of the copolymer as obtained from ellipsometry (scatter plus line) together with the thin-film absorption spectrum (solid line).

considering the classical treatment, one expects an initially linear rise of the phosphorescence intensity, which turns into a square root dependency once bimolecular triplet annihilation becomes the major decay path for the triplet excitons. In Fig. 5, the phosphorescence after the excitation pulse (delay 100 ms) as well as the integrated fluorescence intensity during the pulse are plotted in a double logarithmic fashion. As expected, the fluorescence intensity increases strictly linearly with the pulse length and so does the phosphorescence initially. For the chosen optical excitation flux (30 mW/cm^2), the turnover into the annihilation limited regime occurs at $\sim 20\ \mu s$ excitation pulse length. Subsequently, the triplet density increases clearly slower than the classically expected exponent of 1/2. Instead, one observes an algebraic increase of the phosphorescence intensity, whose exponent fits quite well with 1/2.71, which is the expected dependency for the dispersive bimolecular triplet annihilation rate with an algebraic density dependence of slope 0.71. Thus, the emission dose dependency is self-consistent with the above absorption dose measurements.

Unfortunately, the time dependence and concomitantly also the density dependence of the triplet diffusivity cannot be cast into an explicit analytical expression, although asymptotically a power law with a slope of -1.04 is obeyed in the zero-temperature limit.[24] However, more importantly for the present experimental situation is the initial and intermediate time domain (measured in terms of the attempt-to-jump frequency) as here most of the (in fact few) migration events occur. In this case, due to the lack of an analytical solution, for practical purposes it is common to approximate the time dependence of the diffusion with the help of algebraic decay laws.[20,21,25–27] Although it remained questionable to what extent such a procedure is legitimate,[28] slopes between 0.6 and 0.8 have been reported in the literature, which agrees well with the value of 0.7 found here.[21]

Having established the triplet density dependence of the bimolecular annihilation rate, attention is now focused again on the parameter a, this time with respect to the relative order of λ^{el} and λ^{opt}; compare Fig. 4. Here, one first notes the identical slope for both excitation modes, which is exclusively caused by the triplet excitation dose dependence of γ_{TT}. This implies that λ^{el} is a true constant that, for example, does not depend on the driving voltage. From the excitation density dependence of γ_{TT}, it furthermore follows that any comparison of the optical relative to the electrical values of a is only meaningful at identical triplet generation rates, respectively identical γ_{TT}. This is why in Fig. 4 the electrical *and* optical parameters, a, have been plotted versus their corresponding triplet generation rates, εI_0, rather than, for example, the overall excitation dose. Apparently, even for identical triplet generation rates both datasets are still offset to each other, which implies $\lambda^{el} > \lambda^{opt}$. In fact, identical exciton generation layer thicknesses for both excitation modes would be a surprising coincidence and have already been excluded from a qualitative analysis of Fig. 3. From Fig. 4, one gains $\lambda^{el} = 5.6\lambda^{opt}$ for the copolymer. In repeating the above procedures for the homopolymer, one obtains an algebraic triplet density dependence of γ_{TT} with a slope of 0.51 and $\lambda^{el} = 11.2\lambda^{opt}$.

Up to this point, all of our results are purely relative, and in order to gain absolute values, independently obtained input parameters are required. For example, knowledge of the absolute value of the intersystem crossing rate allows one to determine the singlet-to-triplet branching ratio after electrical excitation.[1] For the present work, we independently measure the value of λ^{opt}, which then yields λ^{el}. Next, using the optical datasets we estimate the value of the constant of proportionality, ε, which yields the triplet-triplet annihilation rate, γ_{TT}.

A determination of λ^{opt} in terms of absorption measurements as a function of concentration using dilute solutions is not accurate enough for the present purpose. Compared to the random, isotropic orientation of the polymer chains in such solutions, the thin-film structure is anisotropic, as the molecules arrange themselves preferably in the plane of the substrate.[14] Instead, the ordinary (perpendicular) absorption component is needed, because in our experimental setup the device is optically excited perpendicular to the sample surface. Here, ellipsometry certainly is the most accurate technique to obtain this quantity. Shown in Fig. 6 are the wavelength-dependent ordinary absorption coefficients that

are obtained by ellipsometry as well as the independently measured thin-film absorption spectra for the copolymer. Apparently, the agreement between the curves is excellent both in shape and energetic position. A similarly good match has also been achieved for the homopolymer. In order to quantify the quality of the fit in common ellipsometry terms, we give the overall mean-square error (MSE), which was calculated from the Woollam software as 3.8 for the copolymer and 5.3 for the homopolymer. Furthermore, an analysis of the correlation matrix confirmed the independence of the ordinary relative to the extraordinary parameters. Thus, the absolute values of the wavelength-dependent optical parameters are reliable to a high degree. From Fig. 6, one infers $\lambda^{opt}=1.15\times10^{7}$ m^{-1} for the copolymer at the laser excitation energy (400 nm). A very similar value was found for the homopolymer, $\lambda^{opt}=1.21\times10^{7}$ m^{-1}. Together with the relative dependencies between optical and electrical absorptivities measured above, the thicknesses of the charge-carrier recombination layers for electrical excitation are found to be $d^{el}=5.1$ and 10.9 nm for the homo- and the copolymer, respectively. Note, these quantities were defined as the sample thickness where the intensity of charge-carrier recombination has dropped to half its maximal value, i.e., $d^{el}=\ln 2/\lambda^{el}$. The uncertainty of these values will be the error of the relative ratio between λ^{opt} and λ^{el}, which is about 5%, plus the error on λ^{opt}. A reasonable estimate for the latter yields about 10%. Therefore, the error margins on the charge-carrier recombination layers are of order 1 nm. The larger charge-carrier recombination layer for the copolymer relative to the homopolymer is well understood on a qualitative level in terms of dissimilar hole mobilities. In addition to an improved hole injection from the ITO anode, the TAD moiety within the copolymer backbone increases the mobility of the holes in this material relative to that of the electrons.[6,11] This implies that, on average, electrons and holes meet each other further away from the anode, which consistently is observed as a wider recombination layer. In fact, this dissimilarity of the hole mobility is the reason why this pair of otherwise very similar polymers was chosen for the present study. Qualitatively, this result can already be inferred from Fig. 4 and as such does not rely on the absolute ellipsometry data. Note, although unlikely, it may be that for the copolymer the hole mobility is so significantly improved that the electron is now the charge carrier with the lower mobility. As a consequence, the recombination zone would be shifted from the anode to the cathode. With only two materials, the present technique is not sensitive enough to distinguish both cases. Nevertheless, this ambiguity can be circumvented by studying a range of smoothly varying materials, for example a series of copolymers with increasing TAD content.

Assuming an injection limited current for our device, which is expected from the fabrication technique,[29] then a comparison between the sample thicknesses and the charge-carrier recombination layer thicknesses suggests a ratio of the electron-to-hole mobilities of ~15 and ~7 for the homo- and the copolymer, respectively. Unfortunately, for conjugated homopolymers so far only hole mobilities have been explicitly measured using the time-of-flight method, thus there is no independent measure for this ratio. However, ratios of about 10 are consistent with general expectations for conjugated homopolymers.[4]

Next, we work out the constant of proportionality of Eq. (5) ε, by estimating the absolute value of I_0 for the copolymer dataset with the highest optical excitation dose. Unlike the measured λ^{opt}, now the absolute values of several parameters are required, therefore this approach can only be considered as an estimate of the order of magnitude rather than a true measurement. Nevertheless, the maximal overall optical laser dose was measured as 48 mW/cm^2. However, due to reflections on the cryostat windows and on the device, only 65% of this flux is absorbed by the active polymer layer. At 400 nm, such an optical flux excites 6.3×10^{20} s^{-1} m^{-2} singlet excitons. For the copolymer in solid state, the fluorescence quantum yield drops to 0.33 at room temperature compared to 0.94 in solution.[18] Assuming that at low temperature this efficiency reaches 0.50 and an inter-system-crossing rate of 0.05,[1] then under the present experimental conditions one estimates 0.025 for the triplet generation yield under present experimental conditions. Employing this value, one arrives at a triplet generation rate flux of 1.6×10^{19} s^{-1} m^{-2}. Combining this rate with the corresponding measured εI_0, 10.3 V s^{-1} (uppermost data point of the optical dataset of Fig. 4), a value for the constant of proportionality of $\varepsilon=6.6\times10^{-19}$ V m^2 is obtained.

Using $a^{opt}(I_0)=\lambda^{opt}\gamma_{TT}(I_0)/\varepsilon$ with λ^{opt} as obtained from ellipsometry and $a^{opt}(I_0)$ derived from Fig. 4, one arrives at an estimate for the triplet-triplet-annihilation rate for the copolymer of $\gamma_{TT}(I_0)=1.1\times10^{-32}I_0^{0.71}$ m^3 s^{-1}. Similarly, for the homopolymer $\gamma_{TT}(I_0)=2.8\times10^{-30}I_0^{0.51}$ m^3 s^{-1} is obtained. Note, in these relations I_0 denotes the triplet generation flux rather than the excitation dose. Thus, for each continuous excitation dose one has an effective (average of the dispersive annihilation rates) annihilation rate. This effective rate may now be compared with annihilation rates that have been derived from quasi-cw photoinduced absorption studies. Before doing so, it might be helpful to calculate some absolute values. For example, if the homopolymer absorbs an excitation flux between 1.5 and 30 mW/cm^2, which correspond to the minimum and maximal absorbed laser power employed here, then the annihilation rate ranges from $\gamma_{TT}=4\times10^{-15}$ to 2×10^{-14} cm^3 s^{-1}. For the same excitation dose, the copolymer values are about one order of magnitude higher and vary from $\gamma_{TT}=6\times10^{-14}$ to $\gamma_{TT}=5\times10^{-13}$ cm^3 s^{-1}. Recently, Ford *et al.* investigated blends of two polyfluorene derivatives by means of quasi-cw photoinduced triplet absorption.[30] These experiments were performed at 10 K, i.e., in the dispersive triplet annihilation regime; thus, one expects an intensity-dependent annihilation rate. However, the authors only considered nondispersive annihilation and thereby obtain annihilation rates of order 10^{-15} cm^3/s.

Another polyfluorene-type copolymer has been investigated by Westerling *et al.* by means of low-temperature time-resolved photoinduced absorption.[31] These authors analyzed some of their work using dispersive annihilation kinetics and in doing so arrived at dispersion parameters between −0.49 and −0.8, which compares well with −0.51 and −0.71 derived here for the homo- and the copolymer, respectively. Also, a value for the time-averaged annihilation constant is given, 2×10^{-15} cm^3/s. However, this value contains some uncertainty, as it depends on the (unknown) absolute value of

the transient triplet absorption cross section. Nevertheless, any comparison of this rate with our results is only meaningful at the same excitation dose. Here, Westerling *et al.* quote a pulse power of 250 $\mu J/cm^2$. If we assume that this dose is focused on 0.25 cm^2, this yields an excitation dose of ~ 1 mW/cm^2. For such a dose, we obtain effective annihilation rates of 3×10^{-15} and 4×10^{-14} cm^3/s for the homo- and the copolymer, respectively. This almost perfect agreement with Westerling's results may be pure coincidence given that different materials were investigated (also our homo- and copolymer values differ by a factor of 10) together with the uncertainties in the triplet generation dose used by Westerling *et al.* Furthermore, similar values are expected only if their material exhibits the same inter-system crossing yield compared to our polymers, such that for identical excitation dose also the triplet generation rate is identical.

In passing, we note that the values for γ_{TT} derived in the present work only apply as long as the triplet diffusion is dispersive for most of the triplet lifetime. It has been shown that increasing temperature induces a turnover from dispersive to nondispersive, i.e., classical, triplet diffusion.[8,21] Here, the critical temperature for polyspirobifluorene derivatives is about 60 K, which has been inferred from temperature-dependent phosphorescence measurements.[19] For nondispersive triplet diffusion, which, for example, applies at room temperature, the triplet annihilation rate is significantly higher as compared to the low-temperature values obtained here. In fact, this impedes almost any triplet observation, either by transient absorption or by phosphorescence detection, in thin films made of pristine conjugated polymers, and this is why throughout the present study low temperature is applied. Nevertheless, the room-temperature triplet annihilation rate will certainly be a true constant rather than a function of the triplet generation dose.

CONCLUSIONS

The present work demonstrates a method to extract valuable information about working electroluminescent devices from an analysis of the low-temperature, time- and, excitation-dose-dependent triplet accumulation following continuous optical and electrical excitation.

As a consequence of the asymmetrical electron and hole mobilities in all common conjugated homopolymers, the charge-carrier recombination takes place in a thin layer close to one of the electrodes. Here, the first real measurement of the thickness of this layer yielded a value of 5 nm for polyspirobifluorene. Also improving the hole mobility toward that of the electrons by means of a built-in hole transport moiety within the polymer backbone is consistently observed as an increase in the recombination layer thickness, which means that both kinds of charge carriers meet each other further away from the anode.

Even at low temperature, triplet accumulation within the device is soon limited by bimolecular triplet annihilation, which in polyspirobifluorene becomes the major decay mechanism for the triplet excitons already with optical excitation doses exceeding about 30 $\mu J/cm^2$. Consistent with the dispersive triplet diffusion at low temperature, an algebraic dependency of γ_{TT} on the triplet generation rate has been observed. Under typical experimental conditions, the low-temperature triplet-triplet annihilation rate is of the order 10^{-14} cm^3 s^{-1}.

ACKNOWLEDGMENTS

The authors would like to thank A. van Dijken and S. Vulto, both from Philips Research Eindhoven, for the devices investigated in this study as well as fruitful discussions. We are thankful to Professor H. Burrows and S. King for measuring the triplet quantum yields and the steady-state absorption spectra. This work was financially supported from CENAMPS, project CEN-04 Photonics Institute.

*Electronic address: carsten.rothe@dur.ac.uk

[1] C. Rothe, S. King, and A. P. Monkman (unpublished).
[2] I. D. Parker, J. Appl. Phys. **75**, 1656 (1994).
[3] A. van Dijken, J. J. A. M. Bastiaansen, N. M. M. Kiggen, B. M. W. Langeveld-Voss, C. Rothe, A. P. Monkman, I. Bach, P. Stößel, and K. Brunner, J. Am. Chem. Soc. **126**, 7718 (2004).
[4] M. Weiter, H. Bassler, V. Gulbinas, and U. Scherf, Chem. Phys. Lett. **379**, 177 (2003).
[5] H. Becker, S. E. Burns, and R. H. Friend, Phys. Rev. B **56**, 1893 (1997).
[6] J. Salbeck, N. Yu, J. Bauer, F. Weissortel, and H. Bestgen, Synth. Met. **91**, 209 (1997).
[7] C. Rothe, S. M. King, F. Dias, and A. P. Monkman, Phys. Rev. B **70**, 195213 (2004).
[8] C. Rothe and A. P. Monkman, Phys. Rev. B **68**, 075208 (2003).
[9] D. Hertel, H. Bassler, R. Guentner, and U. Scherf, J. Chem. Phys. **115**, 10007 (2001).
[10] S. Sinha, C. Rothe, R. Guntner, U. Scherf, and A. P. Monkman, Phys. Rev. Lett. **90**, 127402 (2003).
[11] J. P. Chen, D. Markiewicz, V. Y. Lee, G. Klaerner, R. D. Miller, and J. C. Scott, Synth. Met. **107**, 203 (1999).
[12] F. B. Diaz, M. Maiti, S. Hintschich, and A. P. Monkman, J. Chem. Phys. **122**, 054904 (2005).
[13] A. van Dijken, A. Perro, E. A. Meulenkamp, and K. Brunner, Org. Electron. **4**, 131 (2003).
[14] M. Tammer, R. W. T. Higgins, and A. P. Monkman, J. Appl. Phys. **91**, 4010 (2002).
[15] B. P. Lyons and A. P. Monkman, J. Appl. Phys. **96**, 4735 (2004).
[16] D. J. Griffiths, *Introduction to Electrodynamics* (Prentice Hall, Englewood Cliffs, NJ, 1989).
[17] D. Hertel, S. Setayesh, H. G. Nothofer, U. Scherf, K. Mullen, and H. Bassler, Adv. Mater. (Weinheim, Ger.) **13**, 65 (2001).
[18] M. Reufer, M. Walter, P. Lagoudakis, A. B. Hummel, J. Kolb, H. Roskos, U. Scherf, and J. M. Lupton, Nat. Mater. **4**, 340 (2005).

[19] C. Rothe, K. Brunner, I. Bach, S. Heun, and A. P. Monkman, J. Chem. Phys. **122**, 084706 (2005).
[20] R. Richert, H. Bassler, B. Ries, B. Movaghar, and M. Grunewald, Philos. Mag. Lett. **59**, 95 (1989).
[21] M. Scheidler, B. Cleve, H. Bassler, and P. Thomas, Chem. Phys. Lett. **225**, 431 (1994).
[22] A. P. Monkman, H. D. Burrows, I. Hamblett, and S. Navaratnam, Chem. Phys. Lett. **340**, 467 (2001).
[23] Y. V. Romanovskii, V. I. Arkhipov, and H. Bassler, Phys. Rev. B **64**, 033104 (2001).
[24] B. Ries and H. Bassler, J. Mol. Electron. **3**, 15 (1987).
[25] J. Lange, B. Ries, and H. Bassler, Chem. Phys. **128**, 47 (1988).
[26] R. Richert and H. Bassler, Chem. Phys. Lett. **118**, 235 (1985).
[27] R. Richert and H. Bassler, J. Chem. Phys. **84**, 3567 (1986).
[28] B. Ries, H. Bassler, M. Grunewald, and B. Movaghar, Phys. Rev. B **37**, 5508 (1988).
[29] A. J. Campbell, D. D. C. Bradley, H. Antoniadis, M. Inbasekaran, W. S. W. Wu, and E. P. Woo, Appl. Phys. Lett. **76**, 1734 (2000).
[30] T. A. Ford, I. Avilov, D. Beljonne, and N. C. Greenham, Phys. Rev. B **71**, 125212 (2005).
[31] M. Westerling, C. Vijila, R. Osterbacka, and H. Stubb, Phys. Rev. B **69**, 245201 (2004).